A Phenomenological Study of the Steady-State Current Sheet Speed in a Magnetically Driven Shock Tube

C. T. CHANG

Danish AEC Research Establishment Risö, Roskilde, Denmark

(Z. Naturforsch. **27 a**, 948—955 [1972]; received 5 November 1971)

The discrepancy between the measured steady-state speed of the current sheet and the theoretically predicted value is examined through a detailed analytical and experimental study of the basic assumptions used in the model. It is found phenomenologicaly that the observed deviation at discharge conditions of low voltage and high pressure could be attributed mainly to the spreading of the current-carrying region in time. The deviation occurring at discharge conditions of high voltage and low pressure could be attributed to the possible presence of an ion drag caused by the interaction between the plasma and the electrode surface.

1. Introduction

When one considers the shock tube as a potential tool for the studying of high temperature gasdynamic phenomena such as excitation, ionization, radiation, nuclear reaction, etc., the necessity of generating sufficiently strong shocks is obvious. Considering the case of ionization for example, the required shock speed strictly speaking depends not only on the specific gas concerned, but also on its initial thermodynamic state and needs a detailed statistic mechanic calculation [1–5]. However, an estimate can be made by using the strong shock approximation, thus if V_i is the required shock speed for ionization, m_1 is the mass of the gas particle ahead of the shock, δ is the number of particles that an original particle decomposes and T_i is the characteristic temperature of ionization defined as

$$k T_i = I + D/2 \tag{1}$$

where I and D are the ionization and dissociation energy per original particle, we have

$$m_1 v_i^2 \cong \tfrac{4}{3}\,\delta\,(k T_i)\,. \tag{2}$$

For reference purpose, the shock speed and its corresponding Mach number calculated this way for the completion of the first stage of ionization of some common gases are given here in Table 1.

On the other hand, the maximum shock speed V, attainable theoretically in an idealized diaphragm-type shock tube, is well known to be limited by the available acoustic speed a_4 of the gas in the driving section [6], thus

$$V = (\gamma_1 + 1)\, a_4/(\gamma_4 - 1) \tag{3}$$

where γ_1 and γ_4 are the ratios of the specific heats of the gases in the driven and the driving section respectively. The difficulty of obtaining the required shock speed in a conventional shock tube is evident, and the prospect of using the electromagnetic driving force is great, especially when a light gas, e. g. H_2 or He, has to be used in the driven section.

In an electromagnetically driven shock tube, the driving mechanism is essentially due to the interaction of the current flowing in a thin sheet and its self or applied magnetic field. The role of the contact surface is replaced by the current sheet (visualized sometimes also as a magnetic piston). In order to have a constant speed shock, the current sheet itself must move at a constant speed. Our previous analysis [7] based on the snowplough model [8] and subsequent experiments performed with a shock tube consisting of rail spark gaps demonstrated that this can be accomplished by using a constant voltage energy source [9, 10]. Specifically, for the electrode configuration (broad parallel plates, length, $l = 38$

Table 1. Shock speed required for the first stage of ionization of some common gases.

Gas	Ionization energy in eV per particle	Shock speed in km/sec	Shock Mach number at $T_1 = 300$ deg. K
A	15.76	10	31
He	24.58	39.7	39
H_2	15.84	63.4	48
N_2	19.41	18.8	54

Remark: The ionization energy of N_2 and H_2 are computed on the basis of ionization following complete dissociation.

Reprint requests to Dr. C. T. CHANG, Atomic Energy Commission, Research Establishment Risö, DK-4000 *Roskilde, Denmark.*

cm, width, $b = 8$ cm, gap, $d = 2$ cm, see Fig. 1) and experimental arrangement used in our case, the front of the curent sheet moves essentially at a constant speed after having travelled approximately 20 cm from the driving end of the tube [9]. At the steady state the predicted current sheet speed $\hat{u}_s$,

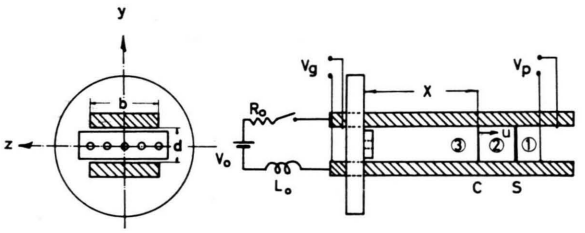

Fig. 1. Schematic drawing of the driving source and the shock tube. Location of the current sheet, the shock and the two voltage dividers are denoted by C, S, V_g and V_p respectively.

regardless of the various discharge conditions of voltage V_0, filling pressure p_1, and the test gas used is related to the driving current $\hat{I}$ *, and the initial density ϱ_1 of the filling gas by the simple expression

$$\hat{u}_s = (L_1/2\,\varrho_1 S)^{1/2}\,\hat{I} \qquad (4)$$

where L_1 and S are the inductance gradient and the enclosed cross sectional area of the electrodes.

To check the expression experimentally, a conventional magnetic probe was inserted at the middle plane of the electrodes, oscillograms of B_z were taken along the various axial positions of the tube. After checked the reproducibility of test runs, a $x-t$ diagram was constructed from the onset times of the B_z traces. The steady-state current sheet speed $\hat{u}$ was then read off from the final linear portion of the trajectory; the corresponding driving current $\hat{I}$ was read from the oscillograms recorded by a Rogowsky belt mounted at the collector plates of the electrodes. The data obtained this way in He for various discharge conditions (V_0, 8 – 13 kV; p_1, 0.020 – 10 Torr) were presented in Figure 2. One observes that the experimental data fall much below the line (a) based on the theoretical value of the inductance gradient $L_1 = \mu(d/b)$ and cannot be fitted completely by a single line with any adjusted value of L_1. However, most of the data obtained from discharge conditions of low voltage and high pressure seem to fit reasonably well on a line with an adjusted value of $L_1 = 0.65$ nH/cm.

* Everywhere in this paper variables with a hat notation refer to their steady-state values.

Denmark.

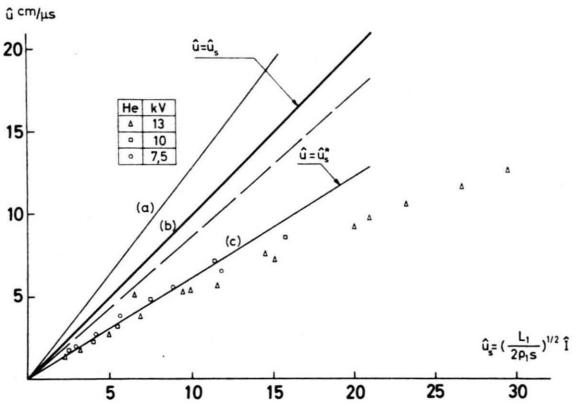

Fig. 2. Variation of the steady-state current sheet speed $\hat{u}$ with respect to the steady-state driving current $\hat{I}$ and the initial gas density ϱ_1. L_1 and S ($= b\,d$) are the inductance gradient and the enclosed cross sectional area of the electrodes respectively. The solid lines are drawn according to the snowplough model, Eq. (4) with (a) $L_1 = 3.14$ nH/cm, (b) $L_1 = 1.8$ nH/cm and (c) $L_1 = L_1^* = 0.65$ nH/cm. The segmented line is drawn according to the "simple shock" theory, Eq. (11), by taking $\eta = 4$.

In view of the statistic nature of the electric breakdown phenomena, the complexity of the plasma surface interactions, the controversy of experimental results obtained by different investigators (l. c. [11–13]), it seems to be fruitless at the present stage of investigation to look for a more elaborate theoretical model to resolve all the discrepancies, instead we shall adopt a phenomenological approach trying to explain these discrepancies within the framework of the original simple model. Such an approach clearly has its severe limitations and cannot avoid being speculative to some extent, nevertheless, it should serve as a useful guide to reveal some possible areas for further exploratory works.

With these considerations in mind, in the following sections we shall present first a brief review of the original theoretical analysis and the fundamental assumptions used; this will be followed by a re-examination of the assumptions by taking some more recent experimental findings and theoretical anlyses into consideration. Finally, using the results derived from analyses, we shall give some plausible explanations regarding the observed discrepancy between the measured and the predicted steady-state speed of the current sheet.

2. Governing Equations and Basic Assumptions

For the convenience of later discussions, it might be worthwhile to restate the governing equations

used in our analysis. Within the framework of the snowplough model the behaviour of the current sheet at any instant is described by its position $x(t)$ along the electrodes, and the current $I(t)$ flowing within the sheet. They are governed by the following equations (see also Fig. 1):

$$\frac{\mathrm{d}}{\mathrm{d}t}\left[(m_0+\varrho_1 S x)\,\dot{x}\right]=\frac{L_1 I^2}{2}, \tag{5}$$

$$V_0=I R_0+(L_0+L_1 x)\,\dot{I}+I L_1 \dot{x}. \tag{6}$$

The physical implications of these equations are self-evident, namely that Eq. (5) implies the conservation of momentum, while Eq. (6) can be looked upon as an energy equation. The first term m_0 on the left-hand side of Eq. (5) represents the mass present at the moment of electric breakdown, the second term represents the mass accumulated by the snowplough. As shown previously [7, 14] this system of equations together with the initial conditions

$$I(0)=0, \quad x(0)=0, \quad \text{and} \quad \dot{x}(0)=0 \tag{7}$$

has a steady-state solution, i. e.

$$\begin{aligned} I \to \hat{I}&=\frac{V_0}{R_0}\frac{(1+4\varepsilon)^{1/2}-1}{2\varepsilon} && \text{for } t \gg L_0/R_0, \\ \dot{x} \to \hat{u}&=\hat{u}_s && \text{for } t \gg L_0/\varepsilon R_0 \end{aligned} \tag{8}$$

where the parameter

$$\varepsilon=\left(\frac{L_1}{R_0}\right)\left(\frac{V_0}{R_0}\right)\left(\frac{L_1}{2\varrho_1 S}\right)^{1/2}=\left(\frac{R_b}{R_0}\right)^2 \tag{9}$$

can be interpreted as the square of the ratio between the "running impedance" R_b of the shock tube and the impedance R_0 of the source.

The main assumptions are:

(1) The end and the side effect of the eletcrodes can be neglected, the lines of force are considered as parallel and straight, and the field is uniform behind the current sheet.

(2) The gas in the volume swept by the current sheet is completely picked up by the sheet.

(3) Plasma impedance is negligible.

(4) The effect of impurities is negligible.

(5) The total current is confined within a thin sheet.

(6) Wall friction plays no significant role.

(7) Ionization efficiency of the sheet is one hundred per cent.

With respect to the model used, assumptions (1), (2), (3), (5), (6) are rather self evident, an explanation concerning the remaining assumptions (4) and (7) might not be superfluous. The presence of impurities could affect the acceleration process in three possible ways:

a) Influence the apparent gas density ϱ_1 of the mass accumulated by the snowplough.

b) Influence the mass m_0 introduced during the electric breakdown.

c) Possible formation of a standing arc near the driving end of the tube especially at discharge conditions of high voltages and low pressures, thus effectively reducing the driving current entering Equation (5).

For the Lorentz force to be effective, the gas being accelerated must be in an ionized state (unless ion neutral collision cross sections are comparatively large). When a current sheet advances into an originally neutral gas, it must, therefore, ionize and trap the incoming gas stream as quickly as possible, a perfect snowplough consequently implies a hundred per cent of ionization efficiency.

3. Re-Examination of the Basic Assumptions

In order to compare the discrepancies between the measured current-sheet speeds and those predicted theoretically, we shall re-examine these assumptions on the basis of further experimental findings and theoretical considerations.

3.1. The Effect of the Finite Width of the Electrodes

The finite width of the electrodes introduces the following effects:

(a) Lowering of the inductance gradient L_1 due to the curvature of magnetic lines of force. This is revealed by the presence of a weak field in front of the main signal of B_z for some discharges. The measured inductance gradient L_1, based on the short-circuit method [10], is only 1.8 nH/cm as compared with 3.14 nH/cm of the theoretical value of $\mu(d/b)$.

(b) "Side pinch" of the current-carrying region. Its possible presence is revealed occasionally in some of the image pictures taken end-on and the sidewise distribution of the current across the electrodes. However, neither experimentally obtained current oscillograms [9] nor theoretical analysis [15] showed that its effect could be of great importance.

3.2. The Finite Compressibility Effect

The snowplough model assumes that all the mass swept by the current sheet is stored in the sheet, and that there is no separation between the shock and the current sheet (hypersonic approximation, $\gamma = 1$). Instead, we can replace it by a"simple shock" model by assuming all the current still flowing in a thin sheet, a region 3 devoid of gas, and a region 2 free of magnetic field (see Fig. 1).

According to the strong shock approximation we have

$$\tfrac{1}{2} u^2 = p_2/(\gamma - 1)\, \varrho_2 . \tag{10}$$

Using the continuity equation to eliminate ϱ_2, and the fact that across the current sheet the magnetic pressure $p_3 = L_1 I^2/2 S$ in region 3 behind the sheet must balance the gas pressure p_2 in region 2, and finally using the hat notation to denote the steady-state, we can write Eq. (10) as

$$\hat{u} = \left[\left(\frac{\eta - 1}{\eta}\right)\left(\frac{L_1}{2\,\varrho_1 S}\right)\right]^{1/2} \hat{I} \tag{11}$$

where $\eta = \varrho_2/\varrho_1$ is the compression ratio. The result is plotted in Fig. 2 for $\eta = 4$. Since $4 \leqq \eta < \infty$, one notices that finite compressibility does reduce the value of $\hat{u}$, but not enough for the observed discrepancy.

3.3. The Plasma Impedance

To check the plasma impedance, we installed two voltage dividers; V_g near the driving end, and V_p near the terminal of the electrodes, see Figure 1. For a discharge voltage around 10 kV, the measured V_p is around 100 V. Comparing it with the measured V_g around 1 kV, and the total current of 100 kA, we find that the plasma impedance is negligible.

3.4. The Effect of Impurities

In a magnetically driven shock tube impurities can be introduced through erosion of cathode material due to sputtering or hot spots, desorption of adsorbed (or absorbed) gas from previous discharges, or ablation of the insulator material at the driving end of the electrodes. Although there is some experimental evidence of electrode erosion, both experimental results and theoretical calculations showed that neither sputtering nor desorption could be of great importance as far as their direct influence on the steady-state speed of the current sheet is concerned [16]. Apart from the effect of increasing the apparent density ϱ_1 of the plasma, the introduction of insulator material into the discharge can also cause the formation of a standing arc near the driving end of the electrodes and thus reduce the effective driving current [12, 17, 18]. To investigate this effect, as shown in Fig. 1, we inserted an alumina spacer (99.9% Al_2O_3) with small holes between the electrodes and carried out some magnetic field measurements near the insulator. Typical oscillograms of B_z obtained in this way are shown here in Figure 3. A comparison between these oscillograms showed that within the experimental range of discharge voltage and pressure used, 7 to

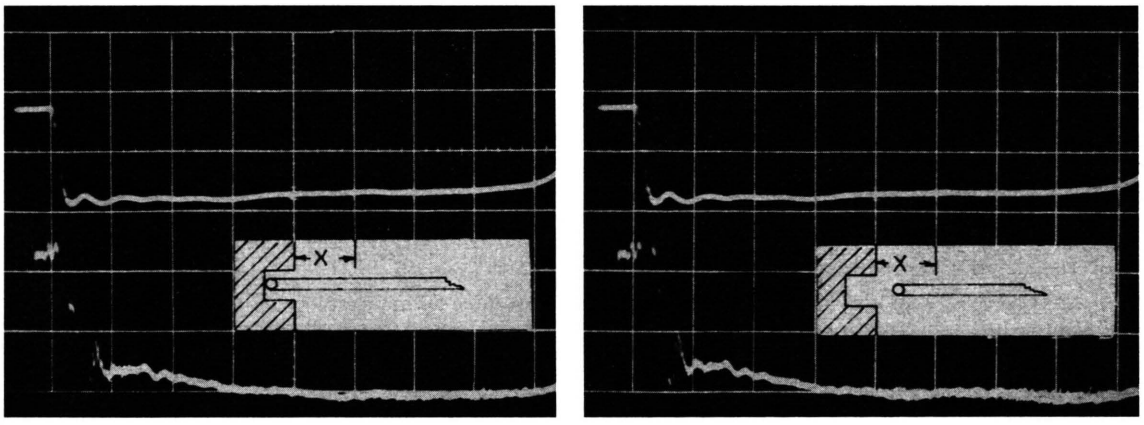

Fig. 3. Representative oscillograms of the total current I (upper trace) and the magnetic field B_z (lower trace) taken in helium discharges, $V_0 = 13$ kV, $P_1 = 0.2$ Torr. The left trace of B_z is obtained with a probe inserted 5 mm inside the insulator spacer; the right one is obtained with a probe placed 10 mm beyond the spacer. Vertical scales: upper trace, 87 kA per div.; lower trace, 0.096 wb/m² per div. Common time scale, 2 μsec per div.

16 kV and 0.1 – 10 Torr, the current flowing near the insulator plate could in no case be more than five per cent of the total amount delivered. Furthermore, image converter photographs taken near the driving end of the tube contrary to the result of an other investigator [19] revealed no standing arc during the running of the current; time and space integrated spectrograms of superimposed discharges revealed no traces of aluminum lines. On the basis of these observations we conclude that ablation of the insulator wall cannot play an important role under our experimental conditions.

3.5. *The Effect of Current Distribution*

According to the argument of ROSENBLUTH [4], the thickness of the current sheet

$$d = \left(\frac{2\, m_e}{\mu\, n_e\, e^2}\right)^{1/2} \tag{12}$$

should vary inversely as the square root of the number density of the electrons, n_e, within the sheet. When n_e is constant in time, the current layer is of constant thickness and moves like a rigid conductor. It can be shown that this will not alter the result given by Equation (2). However, if the current layer spreads in time, this will phenomenologically cause a reduction of the inductance gradient L_1, which according to Eq. (4), will cause a reduction in the current sheet speed [14]. This effect was noticed also by an other investigator [11].

3.6. *The Effect of Wall Friction* [20]

Owing to our limited knowledge of the interaction between plasma and the wall surface, the exact form of the friction F_f is difficult to describe. On account of this, we followed a semi-empirical approach by assuming some plausible forms of F_f and proceeded to analyse its effect numerically. The postulated laws of friction are:

(a) Linear law. When the mean free path of the ions near the wall is large, and a certain fraction of the driving current is carried by ions, we may consider friction as essentially due to the ion drag [21] and write

$$F_f = \beta (I\, m_i/e)\, \dot{x} \tag{13}$$

where the numerical factor β depends on the nature of interaction and can be taken as some positive factor less than unity. At steady-state its effect is equivalent to the introduction of an apparent inductance gradient,

$$L_f = \frac{\beta\, m_i}{e}\left(\frac{L_1}{2\,\varrho_1\, S}\right)^{1/2}. \tag{14}$$

Specifically, the steady-state current-sheet speed is given by

$$\hat{u} = \left\{\left[1 + \left(\frac{L_f}{L_1}\right)^2\right]^{1/2} - \left(\frac{L_f}{L_1}\right)\right\} \cdot \hat{u}_s\,. \tag{15}$$

As a result, the steady-state current-sheet speed $\hat{u}$ strictly speaking no longer scales linearly as the parameter $\hat{I}\,\varrho_1^{-1/2}$ as indicated by the simple snowplough model, Equation (4). However, the deviation is small at lower values of $\hat{I}\,\varrho_1^{-1/2}$ and becomes noticeable only at higher values of $\hat{I}\,\varrho_1^{-1/2}$. This seems to be indicated by experimental data shown in Figure 2.

(b) Quadratic law. When the mean free path of the ions near the wall is small, there might exist a viscous layer near the electrode. We may take

$$F_f = \alpha\, \varrho_1\, S\, \dot{x}^2\,. \tag{16}$$

Other power laws of $\dot{x}$ can also be assumed, but will not alter the result greatly. The net effect on $\hat{u}$ is a reduction of L_1 by a factor $(1+\alpha)$; specifically we have

$$\hat{u} = \left\{\frac{L_1}{2(1+\alpha)\,\varrho_1\, S}\right\}^{1/2} \hat{I}\,. \tag{17}$$

3.7. *The Effect of Ionizing Efficiency*

If we assume that of the n_1 incoming particles which hit the current sheet only a fraction, Θ, interacts with it inelastically, with ν as the average cosine factor for momentum exchange, we can rewrite the momentum equation as

$$\frac{\mathrm{d}}{\mathrm{d}t}\left[(m_0 + \Theta\,\varrho_1\, S\, x)\,\dot{x}\right] + (1-\Theta)\,(1-\nu)\,\varrho_1\, S\,\dot{x}^2 = \frac{L_1 I^2}{2}\,. \tag{18}$$

One notices that when $\Theta = 1$, Eq. (18) reduces to Eq. (5) of the simple snowplough model. When we compare the above equation with the momentum equation including the effect of viscous drag with F_f taken as given by Eq. (16), we observe that it reduces formally to the case already treated if we introduce an apparent density

$$\varrho_1^* = \Theta\,\varrho_1 \tag{19}$$

and an apparent friction coefficient

$$\alpha = (1-\Theta)\,(1-\nu)/\Theta\,. \tag{20}$$

Specifically, the steady-state current-sheet speed is given by

$$\hat{u} = \{L_1/2\,\varrho_1\, S[1-\nu(1-\Theta)]\}^{1/2}\,\hat{I}\,. \tag{21}$$

4. Conclusion and Discussion

After these brief reviews of the theoretical analysis and experimental findings, it might be worthwhile to take a look at the result presented in Fig. 2 again. In view of the fact that no single line can be drawn to fit the experimental data covering the whole range of discharge conditions, one is tempted, at first, to interpret this as an evidence of the presence of an ion drag of the kind described in Section 3.6. A simple calculation shows that this *alone* is not adequate enough to account for the observed discrepancy. In order to fit the data with Eq. (15) either the numerical factor β or the ion mass m_i entering Eq. (14) has to be unrealistically large. On the other hand, one notices that most of the experimental data deduced from discharge conditions of low voltage and high pressure do not lie on the straight line $\hat{u}=\hat{u}_s$, but can be fitted reasonably well on a straight line $\hat{u}=\hat{u}_s{}^*$ with a lower slope. This can be interpreted as meaning that under the experimental conditions the effective inductance gradient $L_1{}^*$ amounts to 0.65 nH/cm only, and not to the measured value of $L_1=1.8$ nH/cm. (We remark here that when the simple shock model is used $L_1=0.98$ nH/cm.)

According to the analysis presented in the previous sections, such a result could be caused by any one or a combination of the following possibilities:

(a) The presence of a viscous drag having a quadratic dependence on the current sheet speed Equation (16);

(b) Poor ionization efficiency, i. e. $\Theta<1$ in Equation (18);

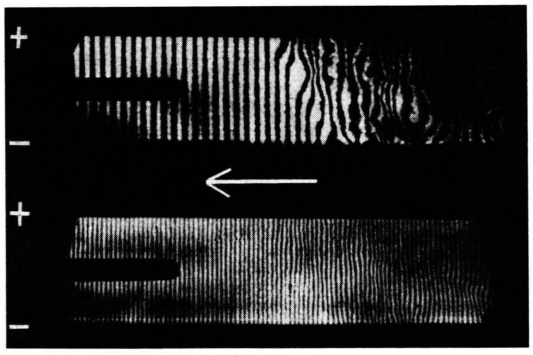

Fig. 4. Differential interferograms taken in helium discharge at 13 kV and 0.5 Torr. The pictures cover an axial position of x from 29 to 36 cm. Direction of motion as indicated by the arrow is from the right to the left. A Q-switched ruby laser is used as the light source. The upper diagram is taken at a wave-length $\lambda=6943$ Å; the lower one at $\lambda=3471$ Å.

(c) Growth of the current layer thickness in time.

Among these possibilities, viscou drag apparently cannot be of great importance under our experimental conditions. This can be seen from the following considerations: the boundary layers as revealed by the differential interferograms are rather thin, Fig. 4; to obtain an effective inductance gradient, $L_1{}^*=0.65$ nH/cm, an unrealistic friction coefficient $\alpha=1.77$ has to be used.

Concerning the other two possibilities, it is difficult to make a clear distinguishing about their relative importance. This is because the real physical cause for the growth of the current layer remains unclear at present.

The growth of the current layer could be caused by the lowering of the electrical conductivity in time or equally well by the ineffective mass accumulation of the magnetic piston (or the current sheet) due to its low ionization efficiency. A leaking piston [22] will leave some plasma behind which will subsequently expand to fill the volume swept by the piston. Following these arguments, possibilities (b) and (c) might very well be both present and reinforce each other. It is quite conceivable that what is found to be the dominating factor in one gas might become of less importance in another. This is particularly true in view of the fact that the ionization efficiency and charge exchange cross sections vary a great deal in different gases [23].

On the other hand, in view of the following observational evidence;

(i) oscillograms of B_z showed a well-defined front, but revealed the existence of a growing wake behind it, see Fig. 5, and

(ii) the time behaviour of the dn_e/dx curve deduced from the smear differential interferograms as the one shown in Fig. 6 showed directly the growth of a current layer, see Fig. 7, (on account of the diffusive nature of the current distribution, we define the thickness of a current layer as the distance between the two consecutive extreme values of the dn_e/dx curve),

we believe that the lowering of the inductance gradient L_1 can be attributed, if not entirely, at least to a great extent by the growth of the current layer in time.

Returning to the remaining experimental data obtained at discharge conditions of high voltage and low pressure, one notices that they deviate definitely from the line $\hat{u}=\hat{u}_s{}^*$. According to the previous

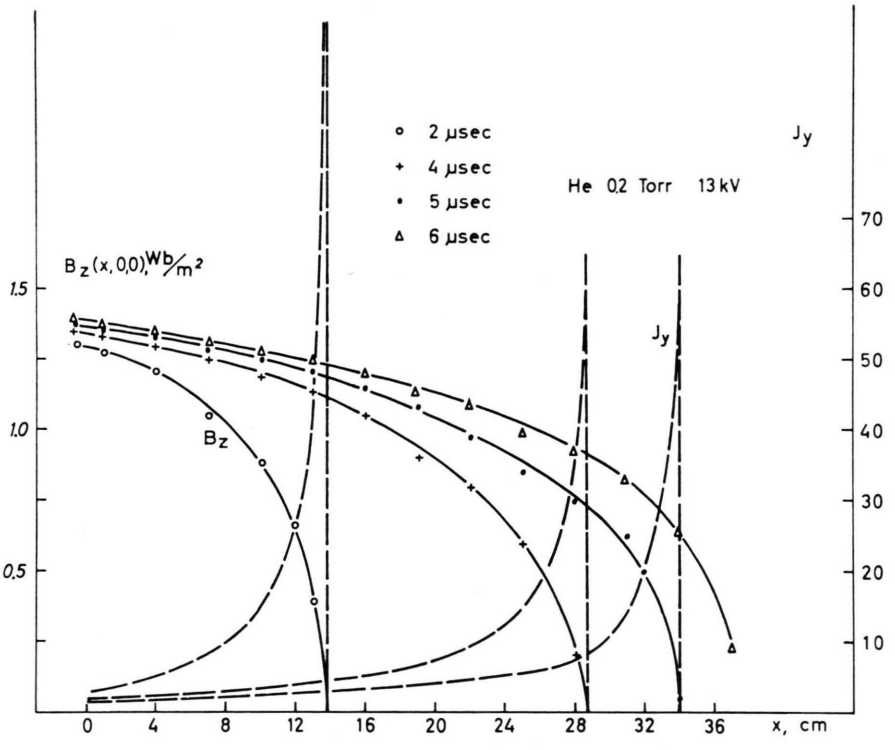

Fig. 5. Variation of $B_z(x, 0, 0)$ and $J_y(x, 0, 0)$ at a given time. Helium discharge at 13 kV a nd 0.2 Torr. The scale of J_y is arbitrary.

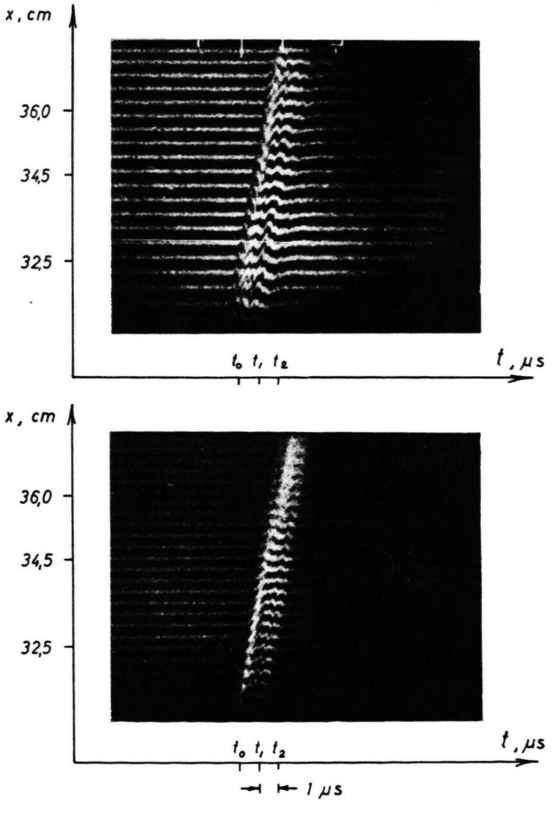

← Fig. 6. Representative smear differential interferograms taken in helium discharge. The upper picture is taken at a wavelength $\lambda = 5461$ Å; the lower one at $\lambda = 4358$ Å. $x = 36$ cm is the end of the electrodes. — Discharge conditiions: 13 kV, 2 Torr.

argument this can be attributed to the presence of an ion drag of the kind given by Eq. (13). (The ion drag could be present under all discharge conditions; however, as we remarked earlier for a reason-

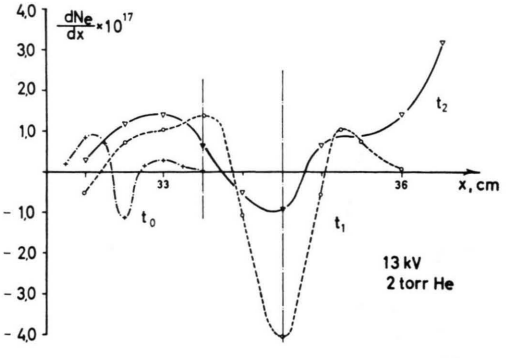

Fig. 7. dn_e/dx profile deduced from the smear differential-interferograms shown in Figure 6. Time origin t_0 is arbitrarily chosen, t_1 and t_2 are taken at 1 and 2 μsec after t_0 respectively. The distance between the two vertical lines indicates the thickness of a current layer as defined in the text at the instant t_1.

able value of β its effect is small at lower values of $\hat{I}\,\varrho_1^{-1/2}$ and becomes noticeable only at higher values of $\hat{I}\,\varrho_1^{-1/2}$.) As an illustration, we took $\beta = 0.43$ replaced L_1 by L_1^*, $\hat{u}_s$ by $\hat{u}_s^*$ in Eqs. (14) and (15) and computed the ratio $\hat{u}/\hat{u}_s^*$ in the pressure range of 20 μ to 2 Torr. The results is shown here in Fig. 8, one notices that the computed curve fits fairly well with the experimental data taken at the discharge voltage $V_0 = 13$ kV.

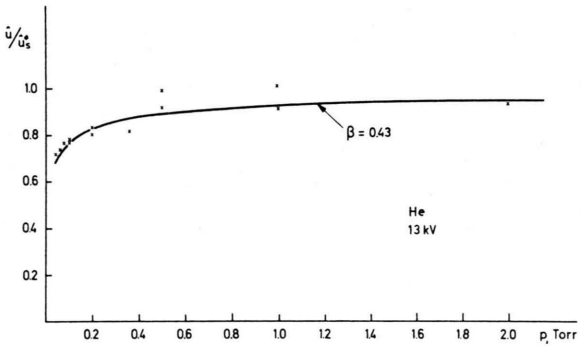

Fig. 8. Variation of the speed ratio $\hat{u}/\hat{u}_s^*$ of the current sheet with respect to the discharge pressure p_1 in the pressure range below 2.0 Torr. $\hat{u}$ is the measured speed derived from the onset time of $B_z(x, 0, 0)$ trace; $\hat{u}_s^*$ is the snowplough speed calculated according to Eq. (4) by taking an adjusted inductance gradient $L_1^* = 0.65$ nH/cm. The curve is drawn according to Equation (15). Experimental data are indicated by crosses.

While the present explanation of the behaviour of the current sheet at discharge conditions of high voltage and low pressure is certainly reasonable, other possibilities should not be excluded. For example, the parameter $\omega_{ce}\,\tau_{ei}$ (where ω_{ce} is the electron cyclotron frequency and τ_{ei} is the electron-ion collision time) under our experimental conditions can be shown to be proportional to I/ϱ_1, consequently the effect of Hall current could very well be of equal or even great importance at these discharge conditions, especially in view of the claims made by other investigators [11, 24–27]. However, as most of our experiments thus far conducted showed (a) no definite correlation of the ratio $\hat{u}/\hat{u}_s^*$ with respect to the discharge voltages at a fixed discharge pressure, (b) no expected variation of the angle of inclination of the current sheet deduced from the differential-interferograms, (an example is given here in Fig. 4), with respect to the discharge pressures at a fixed discharge voltage, it is difficult to draw any definite conclusion regarding its effect under our experimental conditions.

On the other hand, since the presence of Hall current is known to cause the deviation of the flow from the one-dimensional geometry and the introduction of vortices [24, 28, 29], clearly it is an effect to be avoided from the pure application point of view of the shock tubes. Speaking it in another way, its presence could very well limit the possible range of application of the electromagnetically driven shock tubes.

Acknowledgement

The author is much indebted to H. MUNTENBRUCH, Max-Planck-Institut für Plasmaphysik, Garching bei München, for bringing to the author's attention the application of differential interferometry in the study of shock waves. Most of the experimental work reported here was done by M. POPOVIĆ and U. KORSBECH, assisted by B. HURUP HANSEN.

[1] G. B. F. NIBLETT, AWRE Report No. O-70/60, AWRE, Aldermaston, Berks., England 1961.
[2] C. T. CHANG, Risö Report No. 27 [1961].
[3] J. ARTMANN, PPS 102, Bericht aus dem 1. Physikalischen Institut der Technischen Hochschule Aachen 1963.
[4] W. FUCKS and J. ARTMANN, Z. Phys. **172**, 118 [1963].
[5] J. ARTMANN, Z. Naturforsch. **20 a**, 857 [1965].
[6] E. L. RESLER, S. C. LIN and A. KANTROWITZ, J. Appl. Phys. **23**, 1390 [1952].
[7] C. T. CHANG and O. KOFOED-HANSEN, Plasma Phys. **10**, 137 [1968].
[8] M. ROSENBLUTH, R. GARWIN, and A. ROSENBLUTH, Los Alamos Scientific Laboratory Report, Report LA-1850 [1956]; see also article by M. ROSENBLUTH in Risö Report No. 18 [1960].
[9] C. T. CHANG, M. POPOVIĆ, and U. KORSBECH, Shock Tubes, Proc. 7-th Int. Shock Tube Symp. Toronto, Canada 1969 (University of Toronto Press 1970, p. 517).
[10] M. POPOVIĆ, Risö Report No. 206 [1969].
[11] L. LIEBING, Laborbericht IPP-Garching, IPP 3/16 [1963].
[12] JAMES KECK, Phys. Fluids Suppl. **7**, S 16 [1964].
[13] C. T. CHANG, M. POPOVIĆ, and U. KORSBECH, Plasma Phys. **12**, 751 [1970].
[14] C. T. CHANG and K. MONDRUP, Plasma Phys. **10**, 1106 [1968].
[15] C. T. CHANG, U. KORSBECH, and K. MONDRUP, Proc. 6-th Int. Shock Tube Symp., Freiburg i. Br., Germany, 1967. Phys. Fluids Suppl. **I**, I-73 [1969].
[16] C. T. CHANG, M. POPOVIĆ, and U. KORSBECH, Contributed Papers, 9-th Int. Conf. Ioniz. Phenom. Gazes, Bucharest, Rumania 1969, p. 122.
[17] A. DATTNER and J. ENINGER, Phys. Fluids Suppl. **7**, S 41 [1964].
[18] L. LINDBERG and C. T. JACOBSEN, Phys. Fluids Suppl. **7**, S 44 [1964].
[19] T. N. LIE, AIAA J. **8**, 206 [1970].
[20] A more detailed account of the effect of wall friction is to be found in C. T. CHANG, Plasma Phys. **13**, 1067 [1971].
[21] K. THOM, J. NORWOOD, and N. JALUFKA, Phys. Fluids Suppl. **7**, S 67 [1964].
[22] L. LIEBING, Phys. Fluids **6**, 1035 [1963].
[23] SANBORN C. BROWN, Basic Data of Plasma Physics, The M.I.T. Press, Cambridge, Mass. 1959.
[24] W. H. BOSTICK, Phys. Fluids **6**, 1598 [1963].
[25] R. B. JOHANSON, Phys. Fluids **8**, 866 [1965].
[26] W. R. ELLIS and R. G. JAHN, J. Plasma Phys. **3**, 189 [1969].
[27] A. C. ECKBRETH and R. G. JAHN, AIAA J. **8**, 138 [1970].
[28] G. C. OATES, AIAA J. **1**, 2785 [1963].
[29] E. A. WITALIS, Plasma Phys. **13**, 939 [1971].